Ultrafast all-optical switching with low saturation energy via intersubband transitions in GaN/AlN quantum-well waveguides

Yan Li, Anirban Bhattacharyya, Christos Thomidis, Theodore D. Moustakas, and Roberto Paiella

Department of Electrical and Computer Engineering and Photonics Center, Boston University, Boston, MA 02215
rpaiella@bu.edu

Abstract: A fiber-optic pump-probe setup is used to demonstrate all-optical switching based on intersubband cross-absorption modulation in GaN/AlN quantum-well waveguides, with record low values of the required control pulse energy. In particular, a signal modulation depth of 10 dB is obtained with control pulse energies as small as 38 pJ. Such low power requirements for this class of materials are mainly ascribed to an optimized design of the waveguide structure. At the same time, the intersubband absorption fully recovers from the control-pulse-induced saturation on a picosecond time scale, so that these nonlinear waveguide devices are suitable for all-optical switching at bit rates of several hundred Gb/s.

OCIS codes: (190.5970) Semiconductor nonlinear optics including MQW; (230.7370) Waveguides

References and links

1. A. V. Gopal, H. Yoshida, A. Neogi, N. Georgiev, T. Mozume, T. Simoyama, O. Wada, and H. Ishikawa, "Intersubband absorption saturation in InGaAs-AlAsSb quantum wells," IEEE J. Quantum Electron. **38**, 1515-1520 (2002).
2. G. W. Cong, R. Akimoto, K. Akita, T. Hasama, and H. Ishikawa, "Low-saturation-energy-driven ultrafast all-optical switching operation in (CdS/ZnSe)/BeTe intersubband transition," Opt. Express **15**, 12123-12130 (2007).
3. C. Gmachl, H. M. Ng, S.-N. G. Chu, and A. Y. Cho, "Intersubband absorption at λ ~ 1.55 μm in well- and modulation-doped GaN/AlGaN multiple quantum wells with superlattice barriers," Appl. Phys. Lett. **77**, 3722-3724 (2000).
4. N. Iizuka, K. Kaneko, and N. Suzuki, "Near-infrared intersubband absorption in GaN/AlN quantum wells grown by molecular beam epitaxy," Appl. Phys. Lett. **81**, 1803-1805 (2002).
5. R. Rapaport, G. Chen, O. Mitrofanov, C. Gmachl, H. M. Ng, and S. N. G. Chu, "Resonant optical nonlinearities from intersubband transitions in GaN/AlN quantum wells," Appl. Phys. Lett. **83**, 263-265 (2003).
6. J. Hamazaki, S. Matsui, H. Kunugita, K. Ema, H. Kanazawa, T. Tachibana, A. Kikuchi, and K. Kishino, "Ultrafast intersubband relaxation and nonlinear susceptibility at 1.55 μm in GaN/AlN multiple-quantum wells," Appl. Phys. Lett. **84**, 1102-1104 (2004).
7. I. Friel, K. Driscoll, E. Kulenica, M. Dutta, R. Paiella, and T. D. Moustakas, "Investigation of the design parameters of AlN/GaN multiple quantum wells grown by molecular beam epitaxy for intersubband absorption," J. Cryst. Growth. **278**, 387-392 (2005).
8. M. Tchernycheva, L. Nevou, L. Doyennette, F. H. Julien, E. Warde, F. Guillot, E. Monroy, E. Bellet-Amalric, T. Remmele, and M. Albrecht, "Systematic experimental and theoretical investigation of intersubband absorption in GaN/AlN quantum wells," Phys. Rev. B **73**, 125347 (2006).
9. M. Tchernycheva, L. Nevou, L. Doyennette, F. H. Julien, F. Guillot, E. Monroy, T. Remmele, and M. Albrecht, "Electron confinement in strongly coupled GaN/AlN quantum wells," Appl. Phys. Lett. **88**, 153113 (2006).
10. K. Driscoll, A. Bhattacharyya, T. D. Moustakas, R. Paiella, L. Zhou, and D. J. Smith, "Intersubband absorption in AlN/GaN/AlGaN coupled quantum wells," Appl. Phys. Lett. **91**, 141104 (2007).
11. D. Hofstetter, S.-S. Schad, H. Wu, W.J. Schaff, and L.F. Eastman, "GaN/AlN-based quantum-well infrared photodetector for 1.55 μm," Appl. Phys. Lett. **83**, 572-574 (2003).

#88708 - $15.00 USD Received 17 Oct 2007; revised 12 Dec 2007; accepted 13 Dec 2007; published 17 Dec 2007

12. E. Baumann, F.R. Giorgetta, D. Hofstetter, S. Leconte, F. Guillot, E. Bellet-Amalric, and E. Monroy, "Electrically adjustable intersubband absorption of a GaN/AlN superlattice grown on a transistorlike structure," Appl. Phys. Lett. **89**, 101121 (2006).
13. L. Nevou, F. H. Julien, R. Colombelli, F. Guillot, and E. Monroy, "Room-temperature intersubband emission of GaN/AlN quantum wells at λ=2.3 μm," Electron. Lett. **42**, 1308-1309 (2006).
14. N. Iizuka, K. Kaneko, and N. Suzuki, "All-optical switch utilizing intersubband transition in GaN quantum wells," IEEE J. Quantum Electron. **42**, 765-771 (2006).
15. Y. Li, A. Bhattacharyya, C. Thomidis, T. D. Moustakas, and R. Paiella, "Nonlinear optical waveguides based on near-infrared intersubband transitions in GaN/AlN quantum wells," Opt. Express **15**, 5860-5865 (2007).
16. http://www.rsoftdesign.com/products/component_design/BeamPROP/
17. R. Hui, S. Taherion, Y. Wan, J. Li, S. X. Jin, J. Y. Lin, and H. X. Jiang, "GaN-based waveguide devices for long-wavelength optical communications," Appl. Phys. Lett. **82**, 1326-1328 (2003).
18. B. E. A. Saleh and M. C. Teich, *Fundamentals of Photonics* (Wiley, 2007), Chap. 14.
19. Y. Li and R. Paiella, "Intersubband all-optical switching based on Coulomb-induced optical nonlinearities in GaN/AlGaN coupled quantum wells," Semicond. Sci. Technol. **21**, 1105-1110 (2006).
20. G. Sun, J. B. Khurgin, and R. A. Soref, "Nonlinear all-optical GaN/AlGaN multi-quantum-well devices for 100 Gb/s applications at λ = 1.55 μm," Appl. Phys. Lett. **87**, 201108 (2005).

1. Introduction

Ultrafast all-optical modulators and switches capable of operation at data rates of several hundred Gb/s are expected to play a key role in next-generation fiber-optic communication networks, to enable the implementation of basic signal processing functions directly in the optical domain. A promising technology for these applications is that of near-infrared intersubband (ISB) transitions in semiconductor quantum wells (QWs), which provide ultrafast relaxation lifetimes, large optical nonlinearities, and suitability to monolithic integration. QW systems with sufficiently large conduction-band offsets to accommodate ISB transitions at fiber-optic communications wavelengths (down to at least 1.55 μm) include InGaAs/AlAsSb [1], (CdS/ZnSe)/BeTe [2], and GaN/Al(Ga)N QWs [3-15].

The latter system in particular has been the subject of extensive research for ISB device development in the past few years. Desirable features of III-nitride semiconductors in this context include especially fast ISB relaxation lifetimes due to the highly polar nature of (Al)(Ga)N, particularly large conduction-band offsets allowing for ISB transitions at record short wavelengths, and very wide bandgaps precluding interband two-photon absorption of near-infrared light. Recently, ISB absorption has been measured in various GaN/Al(Ga)N isolated [3-8] and coupled [9, 10] QW systems, followed by the initial demonstration of basic device functionalities such as photodetection [11], electroabsorption modulation [12], and optically pumped light emission [13]. All-optical switching based on ISB cross-absorption saturation in ridge-waveguide devices has also been demonstrated [14], with the expected ultrafast recovery times. At the same time, however, relative large values of the required switching energy were reported in these experiments, e.g. control pulses with energy well in excess of 100 pJ were needed to produce a 10-dB modulation depth of the signal transmission.

In a recent paper we have introduced an optimized GaN/AlN QW waveguide design exhibiting strong ISB self-absorption saturation at record low input power levels, as determined from waveguide transmission measurements with a single (pulsed) input wave [15]. Here we use similar devices in a pump-probe configuration to demonstrate ultrafast ISB all-optical switching with pulse energies as low as 38 pJ for 10-dB modulation depth. These results strongly substantiate the promise of ISB transitions in III-nitride QWs for the development of practical high-performance switching devices for future fiber-optic communication networks.

2. Waveguide design, growth, fabrication, and loss measurements

A schematic cross-section of the devices used in this work is shown in Fig. 1(a). The multiple-QW active layer consists of 30 repetitions of 18-Å-thick GaN wells and 40-Å-thick AlN barriers, sandwiched between a 1.5-μm-thick AlN lower cladding layer and a 0.6-μm-thick GaN cap layer. This material was grown by RF plasma-assisted molecular beam epitaxy

#88708 - $15.00 USD Received 17 Oct 2007; revised 12 Dec 2007; accepted 13 Dec 2007; published 17 Dec 2007

(MBE) on a c-plane sapphire substrate, as described in more detail in Ref. [15]. All GaN wells were uniformly doped n-type with Si at a nominal level of $4x10^{19}$ cm^{-3}, in order to populate the ground-state subbands with a large density of electrons.

Ridges of different widths extending through the entire thickness of the GaN cap were then fabricated by inductively-coupled-plasma etching in a chlorine-based chemistry. Bars containing several waveguides were finally separated after scribing through the backside. The resulting devices display sufficiently high-quality facets for optical testing, although a certain amount of misalignment and in some cases roughness are introduced during bar separation due to the lack of common cleavage planes between c-plane sapphire and nitride epitaxial films. To improve the coupling efficiency, a mechanical polishing procedure based on fine diamond powder was also used to smoothen and align the bar facets.

In the waveguide geometry of Fig. 1(a), the optical modes are primarily confined in the higher-index GaN cap layer and in the QWs, while they decay evanescently into the lower-index AlN cladding; to illustrate, a color map of the fundamental TM mode is also shown in the figure. As a result, these modes have negligibly small amplitude at the sapphire-semiconductor interface, where a high density of material structural defects exists which can cause significant optical propagation losses. At the same time, the 0.6-μm thickness of the cap layer (roughly equal to the wavelength of 1.55-μm light in GaN) was selected so as to maximize the overlap factor between the guided modes and the QW active layer. The low transmission-loss saturation power measured in these devices compared to previously reported waveguide structures [14] is largely attributed to these design prescriptions [15].

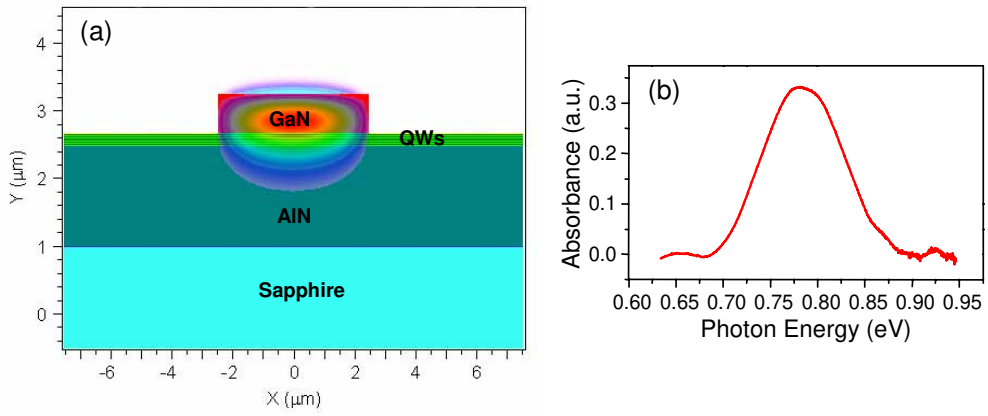

Fig. 1. (a). Schematic cross-section of the GaN/AlN waveguide structure used in this work, and color map of the intensity profile of its fundamental TM mode at 1.55 μm (computed using commercial software based on the beam propagation method [16]). The refractive index values used in this simulation are 1.746 for sapphire, 2.335 for GaN, and 2.031 for AlN [17]. (b) Measured ISB absorption spectrum of the QW active material.

The overall waveguide transmission losses include input and output coupling losses, non-saturable propagation losses due, e.g., to material defects and sidewall roughness, and (for TM-polarized light) saturable losses due to ISB absorption. These mechanisms for the waveguide structure of Fig. 1(a) were studied in detail in Ref. [15]. In particular, the multiple-QW active layer was found to provide a pronounced ISB absorption peak centered at 786 meV (1.58 μm) with full width at half maximum of about 97 meV. This absorption spectrum, as measured via Fourier transform infrared (FTIR) spectroscopy, is shown in Fig. 1(b). The resulting waveguide ISB absorption losses at 1.55 μm amount to about 24 dB/mm in the fully non-saturated regime (i.e. for input power levels well below the ISB absorption saturation power).

Additionally, non-saturable TE (TM) propagation losses of about 2 (4) dB/mm and coupling losses of about 6 dB/facet were measured via the cutback method [15], using

#88708 - $15.00 USD Received 17 Oct 2007; revised 12 Dec 2007; accepted 13 Dec 2007; published 17 Dec 2007

waveguides based on the geometry of Fig. 1(a) but with QWs providing negligible ISB absorption near 1.55 μm. The 2 dB/mm difference between the measured non-saturable TM and TE losses may be ascribed to edge dislocations parallel to the growth axis. These line defects introduce acceptor centers where electrons can be captured, and therefore can effectively act as a wire-grid polarizer [14]. A particularly large density of such structural defects exists within the first few tens of nm of nitride epitaxial material near the sapphire substrate, which explains the importance of spatially separating the guided modes from this region. Additional improvements in the material quality leading to lower dislocation densities in the QWs may help to further reduce these non-saturable polarization-dependent losses.

3. All-optical switching results and discussion

The measurement setup used in this work is shown schematically in Fig. 2. The light source is a passively mode-locked Er-doped fiber laser with 20-MHz repetition rate, peak power of a few hundred Watts, and pulse width of a few hundred femtoseconds depending on the pumping conditions. The laser module provides two fiber-coupled output ports, a high-power port used for the control (pump) wave and a low-power port used for the signal (probe) wave. The two waves are combined with a variable beam splitter/combiner based on free-space polarization optics, and then coupled in and out of the waveguides using tapered fibers placed on 5-axis nanopositioning flexure stages. To demonstrate all-optical switching of the signal by the control wave, the signal transmittance through the waveguide is measured as a function of the signal-control delay time. To that purpose, the signal pulses are passed through a variable delay line with a mechanical chopper running at about 2 kHz inserted in their optical path. The detector photocurrent measured at the waveguide output as a function of the signal-control delay time is then fed into a lock-in amplifier synchronized with the chopper, so as to isolate the signal power from that of the control wave.

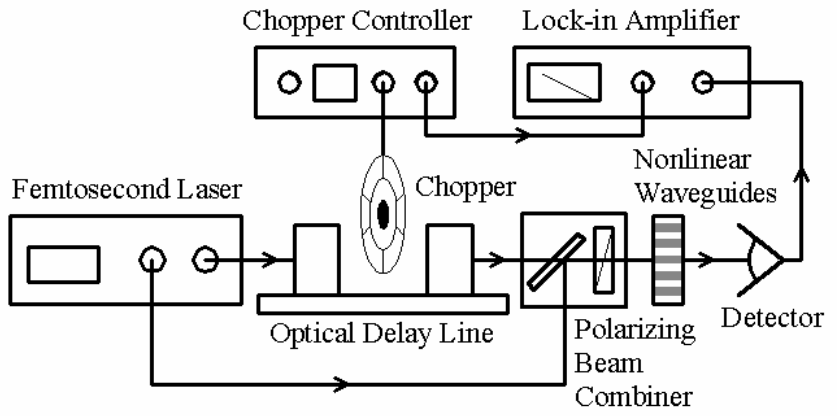

Fig. 2. Pump-probe measurement setup used in this work.

It should be noted that the entire optical circuit used in these measurements is fiber-based. All fiber patch-cords on the input side are polarization maintaining, which allows controlling the polarization of the input waves as required by the selection rules of ISB transitions (i.e. only TM-polarized light is coupled to these transitions). In addition, with the exception of the tapered fiber they are also dispersion shifted so as to avoid excessive broadening of the optical pulses. The temporal width of the control and signal pulses launched into the waveguides is approximately 160 fs, as measured by two-photon-absorption autocorrelation after an identical fiber span.

Shown in Fig. 3(a) is the measured signal transmittance versus signal-control delay time, for different values of the control pulse energy (measured before coupling into the waveguide). In each case the signal pulse energy is smaller than that of the control wave by

#88708 - $15.00 USD Received 17 Oct 2007; revised 12 Dec 2007; accepted 13 Dec 2007; published 17 Dec 2007

about three orders of magnitude. The waveguide used in these measurements is 1-mm long and 3-μm wide; the input pulses are TM polarized, and their spectra are centered at 1550 nm. As clearly illustrated in this figure, when the two input waves are properly synchronized to each other the signal transmittance through the waveguide is very effectively increased by the control pulses via ISB cross-absorption saturation. The resulting signal modulation depth is plotted versus control pulse energy in Fig. 3(b). The switching energy required for 10-dB modulation is about 38 pJ; this value and more in general the data of Fig. 3(b) represent an improvement by a factor of about 4 relative to the best previously reported results in the area of all-optical switching with III-nitride QWs [14]. No modulation of the signal transmittance by the control pulses was obtained when either wave was TE polarized, which confirms the ISB origin of the observed all-optical gating.

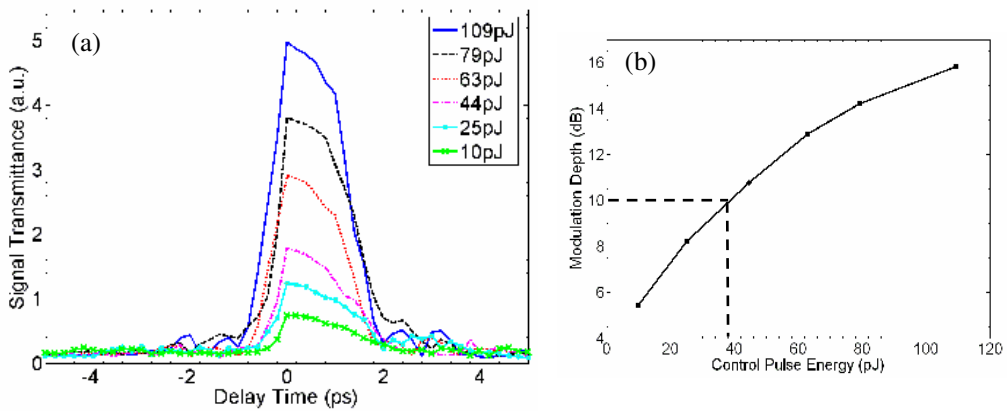

Fig. 3. (a). Transmittance of the signal pulses through a 3-μm-wide, 1-mm-long waveguide versus signal-control delay time, for different values of the control pulse energy. (b) Signal modulation depth (i.e. maximum control-pulse-induced increase in the signal transmittance relative to the fully non-saturated case) versus control pulse energy, as determined from the traces of (a).

Using the known waveguide parameters and a simple model of light propagation in the presence of homogeneously-broadened saturable absorption [18], the measured 10-dB switching input power of (38 pJ)/(160 fs) was found to correspond to a material ISB-absorption saturation intensity I_{sat} of ~ 9.6 W/μm^2. This is in reasonable agreement with the value computed in Ref. [19] for similar GaN/AlN QWs (3.9 W/μm^2), with the difference possibly arising from the presence of inhomogeneous broadening in the absorption spectrum and/or pulse broadening due to dispersion in the waveguide. These values (both experimental and theoretical) correspond to an ISB absorption linewidth Δν of about 100 meV, and can be decreased by improving the material quality to reduce both Δν and the degree of inhomogeneous broadening.

The temporal widths of the traces of Fig. 3(a) are in the range 1.57-1.72 ps (full width at half maximum). These values are affected by a certain degree of timing jitter present in the measurements (ascribed to the laser source), which is also reflected in the shape of the pump-probe traces. Due to this jitter, we cannot infer from the data of Fig. 3(a) the exact value of the ISB absorption relaxation lifetime, which is expected to be in the range of several hundred femtoseconds [5-6]. In any case, the results of our measurements already clearly indicate the suitability of these nonlinear waveguide devices for all-optical gating with switching windows of only a few picoseconds, i.e. at bit rates of several hundred Gb/s.

4. Summary

In conclusion, we have used an all-fiber pump-probe setup to demonstrate all-optical switching at 1.55 μm in GaN/AlN QW waveguides, with record low values of the required

#88708 - $15.00 USD Received 17 Oct 2007; revised 12 Dec 2007; accepted 13 Dec 2007; published 17 Dec 2007

control pulse energy. The demonstrated improvement in this key figure of merit is mainly ascribed to an optimized design of the waveguide structure. Combined with their ultrafast relaxation lifetimes, these III-nitride devices are therefore very promising for the implementation of practical high-performance all-optical switching. Further improvements in the control energy requirements can be achieved by decreasing the ISB absorption saturation intensity I_{sat} of the active material, e.g. through advances in the QW crystal quality leading to narrower ISB absorption linewidths and/or through the use of more complex QW structures [20, 19]. In particular, according to the simulations of Ref. [19] I_{sat} can be decreased by a factor of over 30 using properly designed AlN/GaN/AlGaN coupled QWs. Altogether we can therefore expect that all-optical switching with (sub) picosecond recovery lifetimes and simultaneously control pulse energies near or below one picoJoule can be achieved with this technology.

Acknowledgments

This work was supported by NSF under grant ECS-0622102.

#88708 - $15.00 USD Received 17 Oct 2007; revised 12 Dec 2007; accepted 13 Dec 2007; published 17 Dec 2007